UNDERSTANDING THE DYNAMICS OF URBAN HEAT ISLAND AS A FUNCTION OF DEVELOPMENT REGULATIONS

Vandana SRIVASTAVA[1✉], Alok SHARMA[2], Sanjay Singh JADON[1]

[1]Department of Architecture and Planning, Madhav Institute of Technology and Science, Gwalior, M. P., India
[2]Indian Institute of Travel and Tourism Management, Gwalior, India

Highlights:

- an innovative concept to prognosticate and mitigate the intensity of SUHI;
- correlation of development control regulations with SUHI intensity;
- identification of indicators of development as an impact of development regulations;
- correlation of physical characteristics of urban fabric with the intensity of SUHI.

Abstract. This study is the first-ever attempt to relate the tools of development control like Floor Space Index (FSI/FAR), ground area covered by building footprints (BFs), and proportions/configurations of open areas, with their impact on the surface urban heat island (SUHI) which modulates the air temperatures. In the case of the Indian megacity Mumbai, statistical analysis of the land surface temperatures (LST) and its correlation with the selected development indicators, reveals that for an FSI increase of 1.0 to 1.8 the SUHI is found to be −2.5 °C less and when BFs reduced from 90% to 42% SUHI was also reduced by −2.5 °C. Highrise development with a large plot size is desirable whereas low-rise development with FSI 1.0 on small plot sizes exhibits the highest SUHI. Open spaces without vegetation do not reduce SUHI. The correlation of development regulations with SUHI intensity will help urban planners to make more informed decisions.

1. Introduction

Today 55% of the world's population lives in urban areas, which is expected to grow up to 68% by 2050 as per United Nations projections. Urbanization is a key contributor to which modulates urban climate (Farid et al., 2022). Rapid urbanisation is harming the thermal environment in urban areas (Shahfahad et al., 2022). Due to Urban Heat Island (UHI), the city core areas experience higher air temperatures than the surrounding rural areas. Many studies have assessed the intensity of UHI with the help of existing weather stations. In India the spatial distribution of weather stations is non-uniform and inadequate, creating large unmonitored land pockets.

Surface heat island is the warming of land surface temperatures (LST), which is measured by the thermal infrared sensors (TIRS) using Quantum Well Infrared Photodetectors (QWIPs) mounted on satellites, in terms of the amount of longwave thermal radiations emitted by the land surface, through remote sensing (Leal Filho et al., 2021; Ogashawara & Bastos, 2012). The intensity of the radiations emitted depends on the LST. The TIRS QWIPs are sensitive to two TIR bands, enabling the separation of the temperature of the earth's surface and atmosphere (Department of the Interior U.S. Geological Survey, 2016). Landsat products find maximum application for the estimation of LST and LULC) (de Almeida et al., 2021). Landsat 8 TIRS channels, with 100 m resolution, are suitable for the analysis of surface thermal variations at the spatial scale appropriate to study the impact of the changes in physical characteristics of the components of the urban fabric and urban geometries (Keeratikasikorn & Bonafoni, 2018).

Earlier studies reveal that the process of urbanization has a significant impact on the lower levels of the atmosphere (Sajjad et al., 2009). At lower levels of the atmosphere, LST is strongly related to air temperatures since it is in direct contact with land surfaces (Schwarz et al., 2012). In an earlier study, it was concluded that temperatures of the surfaces found in the surroundings, weighted by the distance, determine the temperature of the air parcel lo-

cated at a given point (Unger et al., 2009). In urban areas, the transformation of land from vegetation to built-up results in an increase in LST (Koko et al., 2021; Sharma et al., 2013). The intensity of SUHI is the difference in LST in an urban area to the LST in rural areas at its fringe. It is found to be positively related to the city's urban spread and population density (Li et al., 2019). Urban areas have an overall flatter horizontal temperature gradient, but they also include isolated regions of abnormally high or low building density, which are linked to warm or cool places (Oke, 1982). The regions with compactly arranged buildings, mid to high rise were found vulnerable to urban heat (Zhang et al., 2023). In low-rise and middle-rise blocks, vegetation and buildings have an impact on LST, whereas in high-rise blocks, buildings are the main contributor (Han et al., 2023).

Previous research has concluded that the built-up areas have a strong positive correlation with the LST (Naim & Kafy, 2021). Vegetation cover is found to have a strong negative correlation with LST (Kalota, 2017; Pan, 2016). An increase in green cover can significantly mitigate the SUHII (Xu, 2015; Wang et al., 2019; Kalota, 2017; Pan, 2016). A recent study also reported a negative correlation between the Normalised Difference Vegetation Index (NDVI) and LST (Gkatzioura & Perakis, 2022; Pandey et al., 2023). Increasing impervious surfaces results in higher SUHI (Ishola et al., 2016). The study conducted in Wuhan concluded that two-dimensional morphology has a greater impact as compared to three-dimensional morphology in modulating LST (Huang & Wang, 2019). A recent study concluded that among the three components of urban spatial form namely landscape pattern, building morphology, and social development, the building morphology is the highest contributor to LST (Chen et al., 2023). The tall buildings with a greater H/W ratio were found to have a negative correlation with the LST (Agathangelidis et al., 2020). To-

gether, building height and building density (Building density is often expressed as the ratio of the total floor area of buildings to the total land area, which is similar to FSI but often expressed in percentage) determines how closely the buildings exist account for almost 75% of the variation in LST (Han et al., 2022). In recent research, wind speed was found to exhibit an inverse relationship with SUHI (Moazzam et al., 2022). Therefore, to manage urban growth in an environmentally responsible way, more studies are required which can help planners in their decision-making (Roy & Kasemi, 2021; Hasnine & Rukhsana, 2020).

The research hypothesises that the tools of development control which lead to achieving higher density of built environment, result in higher intensity of surface urban heat island. Therefore, this research aims to relate the tools of development control like FSI/FAR, ground area covered by BFs, and proportions/configurations of open areas, with their impact on the SUHI. The following objectives are outlined:

1. In the larger study area of the Mumbai Metropolitan Region (MMR) identifying the zones that exhibit homogeneity in the physical characteristics and spatial distribution of various components of urban fabric.
2. To relate the physical characteristics as the indicators of development with the regulations of development control applicable as per local DCR.
3. To identify and analyse the relative impact of the selected indicators on the spatial distribution of SUHI intensities.

2. Methodology

Physical characteristics are identified in terms of indicators such as the proportion of vegetative surfaces, open areas, street widths, plot sizes, the ground covered by BFs,
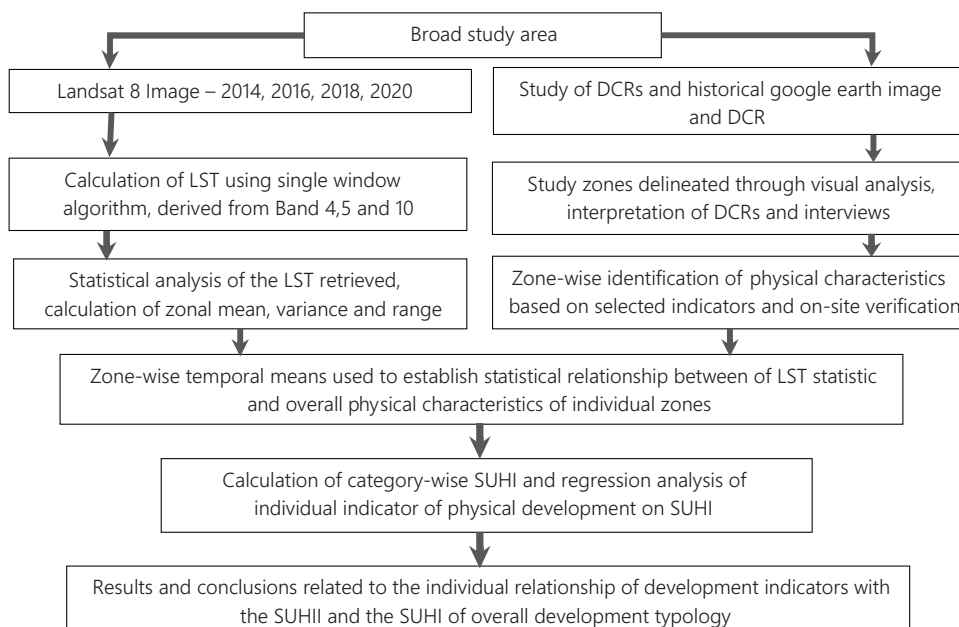

Figure 1. Methodology flow chart

number of floors, floor space index (FSI) and materials, which are largely an outcome of the land use allocations in the development plans (DP) and development control regulations (DCR) applicable in the area. Figure 1 shows the flow diagram of the methodology of the study conducted. Within the broad study area of the Mumbai Metropolitan Region (MMR) pockets of development were identified and delineated, which exhibit, distinct and homogeneous physical characteristics based on the selected indicators. A study of past and present local DCRs, interviews of the professionals and on-site surveys were conducted to understand the physical development in these study zones. The average values of the indicators were calculated (Table 2). From the Landsat 8 data acquired as discussed in 3.2, LST was retrieved using the single window algorithm as done in a similar study for comparing LULC change and its impact on LST in two urban areas in India namely Surat and Bharuch (Mukherjee & Singh, 2020). The zonal mean of LST was calculated for each zone in QGIS. The zonal mean of LST (ZMLST) was then used to calculate SUHI in the zone. A further statistical relationship was worked out between the FSI and SUHII.

3. Study area

The study focuses on the identified pockets of residential development, from a larger study area of one of the most densely populated Indian Megacities, Mumbai (latitude is 19.076090, longitude is 72.877426) along with its suburbs and exurbs in the state of Maharashtra (Figures 2, 3 and 4). Mumbai is 12 m above sea level. The climate of Mumbai is described as Tropical, Wet and Dry Climate, which is moderately hot with high levels of humidity. According to Köppen and Geiger, this climate is classified as Aw. The average annual temperature is 26.4 °C. The temperature variation throughout the year is less owing to its tropical location and is situated on the western sea coast.
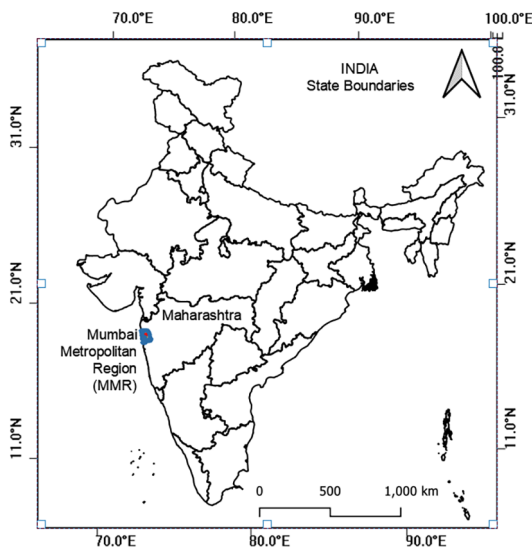
The warmest month of the year is May, with an average temperature of 29.0 °C. At 23.9 °C. January is the coldest month of the year (source: Climate Data, n.d.)

The urban fabric of Mumbai has historically evolved from a group of seven islands to the current metropolitan region of 6355 sqkm, with a population of over 26 million. It incorporates various zones of development that exhibit uniform and distinct physical, social and economic characteristics and which are largely an outcome of local DCRs and other forces acting over a longer timeline of the past. In an attempt to quantify UHI dynamics of Mumbai concerning the LU/LC change, using Landsat datasets it was found that there was a decline of 40% in the vegetation cover whereas the built-up areas almost doubled during 1991–2018 (Shahfahad et al., 2021).
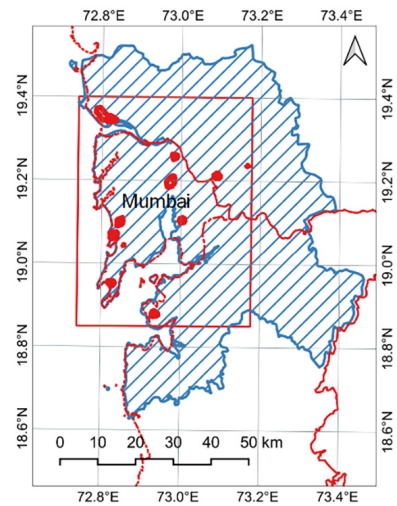
Figure 3. Shows MMR with the outline of large study area (source: Mumbai Metropolitan Region Development Authority, n.d.)

Figure 2. Map showing location of larger study area of MMR within the state of Maharashtra, India
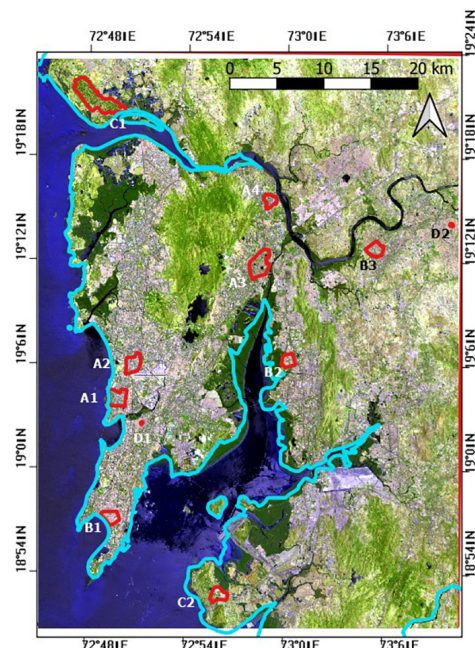
Figure 4. Shows the identified study zones in the study area within MMR

3.1. Category-wise selection of zones

As in the case of previous research (Parvez et al., 2021), the pockets of residential development were identified from the satellite image of the broad study area (Figure 3), acquired from Google Earth, on March 13, 2021. The selection of study zones was based on visual perception and analysis of the grain, colour, and texture of the satellite image which represents different forms of urban development. A similar methodology was adopted to understand LULC in a study of surface temperatures in Delhi (Singh et al., 2014). These zones exhibit homogeneity in terms of the physical parameters like the proportions of built and unbuilt, vegetated/non-vegetated areas, height and compactness of built forms and their roofing materials. The study of DCRs, interviews of the professionals and on-site surveys concluded that the existing residential development can be categorized into four major types of development A to D (Figure 5 and Figure 6) which are:

(A) Highrise buildings: Here average plot size is big (more than 4000 sqm) and the FSI permissible is around 2.0 (±0.5), with wide road abutting, having provision of a large recreational ground (RG). Marginal open spaces (MOS) are wider up to 10–12 m. To fulfil this criterion and consume full FSI, the developers have to build higher floors (8 & above with a height of more than 24 m) which in addition invites stringent firefighting regulations for the movement of firefighting vehicles. In the present study, category "A" includes Bandra West (A1) and Vile Parle (A2) in the main city of Mumbai and old city area (A3) and the newly developed township (A4) in the eastern suburb of Thane.

(B) Midrise buildings: Here average plot size is less than 4000 sqm, FSI is around 1.0 (±0.25), and the abutting road is less than 12.0 m. The number of floors, in this case, is a maximum of up to 8 (24 m), since beyond 24 m provision of refuge area is required, RG is not required due to the smaller plot size, hence only MOS is required. Construction is dense, vegetation is mostly along the roadside and in the MOS. In the present study, category "B" includes the very old development of Kalbadevi opposite Chhatrapati Shivaji Railway Terminus (B1), Kopakhairane in Navi Mumbai (B2) and the satellite town of Dombivli (B3).

(C) Low rise in suburbs/exurbs: Rural area with average plots being small, housing single family, large plots have vegetation and are undeveloped, although FSI is up to 1.0 but remains utilized, construction activity as an urban sprawl of Mumbai is not seen, roads are narrow (up to 6 m), the number of floors is usually 3 to 4. In the present study, category "C" includes the twin towns of Vasai Virar (C1) in the north and Uran in the south (C2) both situated at the fringe of the city.

(D) Low-rise housing for the economically weaker section: Such development is usually planned outside the core area of the city, which eventually becomes a part of the city. FSI consumed is around 1.0, roads here are very narrow and even non-existent; maximum height is up to 5 floors (15 m). Roofs are normally covered with metal sheets. In the present study, category "D" includes low rise, high-density, slum area of Dharavi (D1) and the old, organic development in Kalyan (D2).

Similar terminology for the classification of buildings was adopted in a study of three-dimensional urban expansion in Lanzhou, China (He et al., 2019).

3.2. Acquiring Landsat 8 datasets

The Geospatial dataset of the study area was retrieved from the Earth Explorer (https://earthexplorer.usgs.gov) which is the data portal of the United States Geological Survey (USGS). The images from Landsat 8, which carries the Operational Land Imager (OLI) and the Thermal Infrared Sensor (TIRS) instruments were selected from Level 2, Collection 2 (for improved geometric accuracies). Collection 2 Landsat 8 L2SP is generated at a 30-meter spatial resolution on a Universal Transverse Mercator (UTM). The TIRS sensor collects image data for two thermal bands with a 100 m spatial resolution of a 190 km swath.

In the studies it was found that the SUHI is most significant in the hottest period of summer (Singh et al., 2014) which is in the month of April-May in the study case, therefore, the following datasets from path 148, row 47, available with less than 10% cloud cover in this time slot
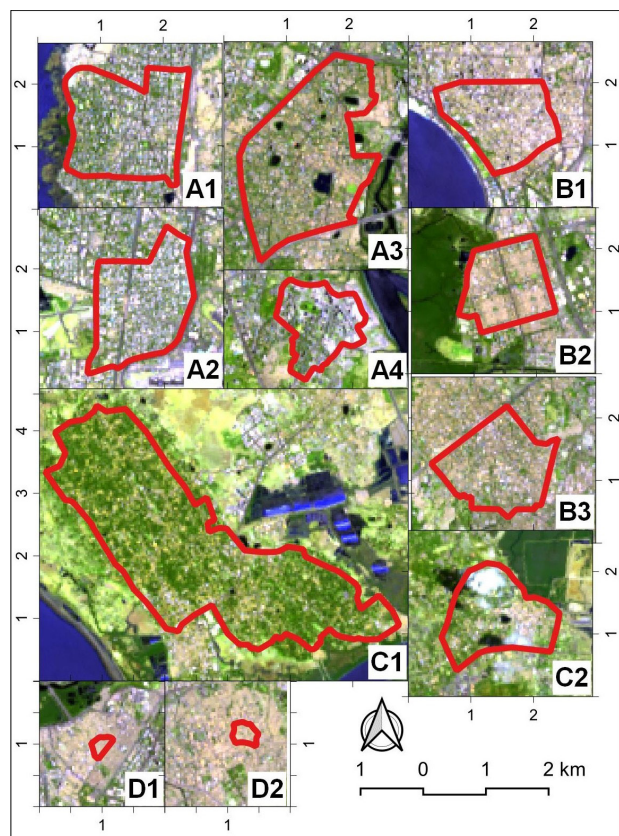
Note: The accuracy assessment of selected zones was calculated based on similarity within the zone. A1 – 93%, A2 – 98%, A3 – 87%, A4 – 90%, B1 – 92%, B2 – 96%, B3 – 97%, C1 – 99%, C2 – 90%, D1 – 98%, D2 – 98%.

Figure 5. Study zones selected under each category
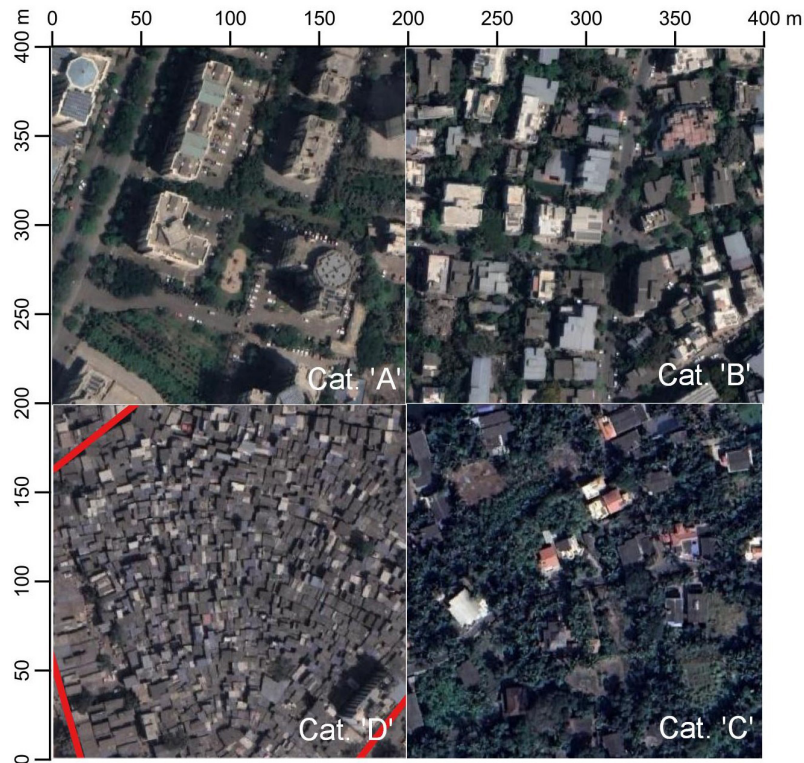
Figure 6. Representative images of the part of urban fabric for categories A, B, C, and D (clockwise from top left) for a sample size of 250×250 m

for the year 2014, 2016, 2018 and 2020 were selected for analysis.

3.3. Calculation of LST

The single window algorithm was used for calculating LST from LANDSAT 8 TIRS which was derived using the observed thermal radiance of the TIRS Band 10 of LANDSAT 8 TIRS. In this algorithm to estimate brightness temperature

(BT), the thermal infrared (TIR) band 10, having a resolution of 100 m was used and for calculating the normalised differential vegetative index (NDVI), bands 4 and 5 with a resolution of 30 m were used. Many researchers have used this algorithm in Landsat 8 satellite data-based studies (Avdan & Jovanovska, 2016). LST was calculated for all four datasets acquired for the years 2014, 2016, 2018 and 2020 in QGIS 3.16.5.

4. Results

4.1. Land Surface Temperatures (LST)

The algorithm used for the calculation of LST is specific for LANDSAT 8 data because of the data complexity (Avdan & Jovanovska, 2016). Figure 7 shows the LST maps of 2014, 2016, 2018 and 2020 respectively.

The LST data retrieved for some of the zones in particular time slots eg. A1-2016, A3-2014, B1-2014 and B3-2014, was discarded as the readings were found to be affected by the presence of clouds. The zone-wise LST and the related statistics as shown in Table 1, were then, re-calculated after removing such readings for conducting further analysis.

4.2. Development indicators

The indicators of development (see Table 2) such as Floor Space Index (FSI), ground coverage or BF, the average size of plots, number of floors, street widths, vegetation

Table 1. Statement of zone-wise mean land surface temperature and related statistics

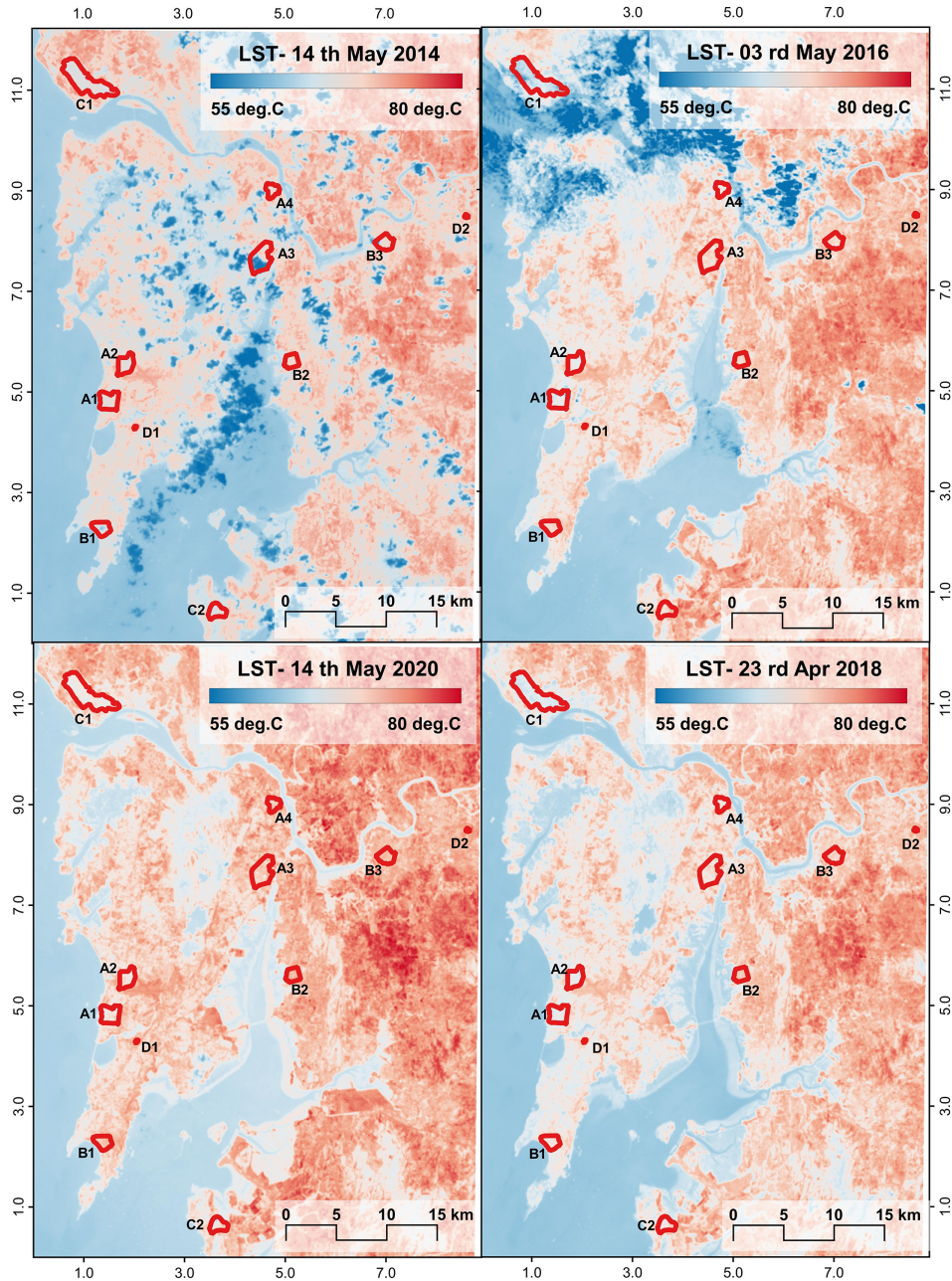| Category/ Zone Id	TM of ZMLST	TVM in °C	TRM in °C	SUHI w.r.t. C1 in °C
I	II	III	IV	V
A/A1	67.9	0.9	6.4	−0.6
A/A2	68.4	1.6	6.1	0.7
A/A3	70.2	1.5	9.2	2.9
A/A4	69.7	1.7	7.3	2.1
B/B1	69.0	4.8	9.3	1.7
B/B2	70.2	1.7	7.1	2.5
B/B3	70.7	0.6	5.2	3.5
C/C1	67.7	4.4	12.6	0.0
C/C2	68.8	1.6	7.1	1.1
D/D1	71.4	0.2	1.8	3.7
D/D2	71.6	0.1	1.4	3.9

Figure 7. LST map of study area for the selected day of year 2014, 2016, 2018 and 2020 (clockwise from top left)

proportion, and roofing materials, were analysed for their correlation on the zonal mean LST.

5. Discussion and interpretations

5.1. Correlation of statistical data with physical characteristics

5.1.1. Analysis of temporal mean (TM) of the zonal mean of LST (ZMLST)

The overall increase of 2.54 °C in LST from 2014 to 2020 is attributed to the reduction in vegetation and densification of built forms over the years. This corresponds to
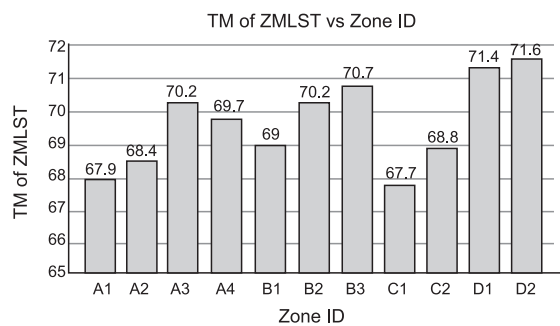

Figure 8. Graph showing the zonal mean of LST in °C on Y-axis, and identified study zones under all categories A-D on X-axis

Table 2. Zone-wise development indicators and typical characteristics of urban development under categories A to D (source: primary survey, interviews and DCRs applicable)

Zone Id	FSI achieved	Building footprint %	Avg. plot size	Average number of floors
I	II	III	IV	V
A1	1.33+TDR= up to 2.7	50	Medium	High rise (10 to 12),
				New (15 to 20 or more)
A2	1.33+TDR= up to 1.5	40	Medium	Midrise (7–8), High rise
				(12–15), airport height restrictions
A3	1.0	50	Medium	Midrise (7 to 8)
A4	1 + TDR = up to 2.0	35	Large	High rise (12 to 34)
B1	No FSI Regulation, up to 3.0	80	Small	Low rise (3 to 5) & midrise (6 to 7)
B2	1.0	80	Small	Low rise (2 to 3)
B3	1.0+TDR (0.8) =1.8 up to 2.0	65–80	Small	Low rise (2 to 4) & midrise (7 to 8)
C1	1.0	30–35	Small	Low rise (2 to 3)
C2	1.0	30–40	Small	Low rise (2 to 5)
D1	1.33	90–95	Very Small	Low rise (1 to 3)
D2	1.33	85–90	Very Small	Low rise (1 to 4)

Zone Id	Vegetation proportion	MOS	Community open spaces	Roofing materials
VI	VII	VIII	IX	X
A1	Medium	Existent	Negligible	Cement concrete
A2	Medium	Existent	Negligible	Cement concrete
A3	Medium	Existent	Small & less in numbers	Mostly terraces are covered with metal sheet roofing
A4	High & well vegetated	Large	Large & well Vegetated	Ceramic tile cool roof
B1	Negligible	Non-existent	Non-existent	Old structures have terracotta tiles whereas new buildings have a metal sheet or concrete roofs
B2	Less	Non-existent	Negligible	All buildings have metal sheet roof
B3	Less	Narrow	Negligible	Metal sheet & cement concrete
C1	High	Narrow	Many plots are undeveloped	Metal sheet & cement concrete
C2	High	Narrow	Many plots are undeveloped	Metal sheet & cement concrete
D1	Nil	Non-existent	Non-existent	All roofs are of metal sheets
D2	Nil	Non-existent	Non-existent	All roofs are of metal sheet

the conclusions of an earlier study of Mumbai City which concluded that there is a 3-fold increase in the LST from 1998 to 2018 (Rahaman et al., 2021). Many plots that were vegetated in 2014 have buildings constructed in 2020.

Under the category "A", the LST is highest in A3 (Figure 8) due to a relatively larger proportion of midrise structures and higher BFs, which leads to more impervious surfaces. This is consistent with the findings of a study of 10 Italian cities which concluded that daytime SUHI increases with the increase in impervious surfaces and a decrease in tree cover (Morabito et al., 2021). Although A4 exhibits large open spaces, the development is still in process, the open spaces are not vegetated, resulting in a higher LST. This is consistent with the findings of previous research, where LST was reported to be high in the barren regions (Pandey et al., 2022b) and low in the thick vegetation cover regions (Suresh et al., 2016). Among A1 and
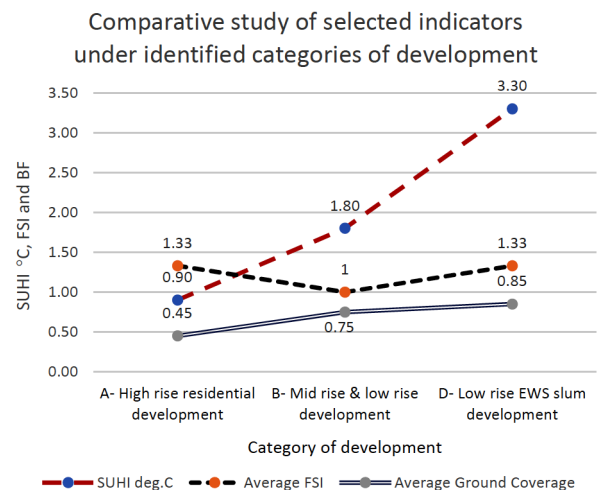
Figure 9. Graph showing category-wise mean of LST, FSI and BFs

A2, having similar physical characteristics, A2 has height restrictions due to its proximity to the airport. The revised DCR with additional TDR was not implemented in A2. In A1 many plots have been redeveloped with additional floors and the lesser ground covered by the BF, making more land free for vegetation, resulting in lower LST which is in agreement with the findings of previous studies. Variation of LST primarily depends upon the land surface materials (Pandey et al., 2022a). Under category "B", the lowest LST for B1 (Figure 8) is attributed to the roofing material being Terracotta/Mangalore tiles (Lesado, 2018), despite the negligible vegetation and high FSI achieved. This phenomenon was observed in a study which concluded that clay tiles perform as a cool roof in their natural albedo (Lesado, 2018).

5.1.2. Analysis of temporal variance mean (TVM)

Under the category "A", the lowest TVM of A1 is due to large plot sizes which allow the impact of vegetation to be significantly transformed as the variation in the surface temperature within the zone. This is supported by the findings of previous research, which suggests that the cooling impact of green space is proportionate to its overall size (Nor Afzan Buyadi et al., 2014). Under category "B", the highest TVM of B1 is due to the large vegetated patches of land cover at the edge of the selected zone towards Marine Drive. The lowest TVM of B3 is due to the fairly homogeneous distribution of the components of urban fabric over relatively smaller plots of land. TVM across category "D" is negligible owing to the uniform land cover without any vegetation or any other landscape feature.

5.1.3. Analysis of temporal range mean (TRM)

Under the category "A", the higher range in A3 can be attributed to the presence of a large number of waterbodies which was also reported in a study earlier which concluded that the water bodies exhibit lower temperatures (Grover & Singh, 2015; Mondal et al., 2021).

Under category "C", C1 displays high TRM due to large patches of dense vegetation that produce a cooling effect and on the other hand, the buildings have metal sheet roof coverings that exhibit high surface temperatures. Category "D" shows the lowest TRM among all the categories, since around 90% of the land is covered by built structures with negligible vegetation. This zone completely lacks cool surfaces like vegetation and waterbodies.

5.2. Category-wise correlation of statistical data with physical characteristics
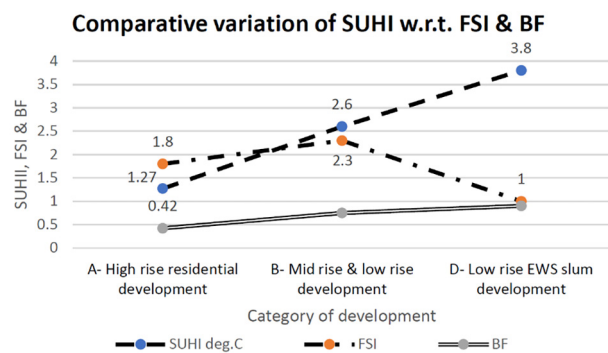
Category-wise comparative statement of LST concerning the physical development indicators reveals that the lowest LST was measured in category "C", of low-rise, low-density residential areas, located beyond the city fringe/exurbs, where the development is still largely rural and the density and type of construction is still unaffected by the city functions (Table 3 and Figure 9). In this zone, the vegetated land cover is up to 65% with a large number of plots being undeveloped.

Table 3 shows the category-wise statements of LST, SUHI, FSI and BF. Among categories, A to D, category "D" which is low-rise development with no vegetation in the area and temporary metal sheet roof coverings, shows the highest LST, whereas category A1 with the highest FSI achieved and least area of ground occupied by BFs shows minimum LST (Figure 9). This phenomenon corresponds to the findings of an earlier study which concludes that two-dimensional morphology (low-rise with larger BF) has a greater impact on LST as compared to 3-dimensional morphology (high-rise with smaller BF) (Huang & Wang, 2019).

In the study, it was observed that the LST calculated for various zones is extremely high compared to the highest air temperatures recorded in the city. This phenomenon was also noted in many earlier research (Avdan & Jovanovska, 2016).

SUHI is defined as the difference in the surface temperatures of urban and rural areas. It is calculated as

$$SUHI = LST(urban) - LST(rural).$$

For this study, zone C1 under Category "C" located at the northern fringe with a low-rise, low-density development is considered as the base case for the calculation of SUHI (Figure 8). It is largely unaffected by the city func-

Figure 10. Graph showing category-wise zonal mean FSI, BF and SUHI as compared to the base case C1

Table 3. Category-wise statement of LST, SUHI, FSI/FAR, building footprints (BF), plot size and Vegetation proportion

Cat.	Cat. mean LST in °C	SUHI in °C	Avg. FSI achieved	Overall BF in %	Avg. plot size	Vegetation proportion
I	II	III	IV	V	VI	VII
A	69.1	1.3	1.8	42	Medium	Medium to high
B	70.0	2.6	2.3	75	Small	Less
C	68.2	1.1	0.4	20	Small	High
D	71.5	3.8	1.0	90	Very small	Negligible

tions having up to 75% vegetated surface, mostly banana and coconut plantations.

All other categories form a part of the urban fabric of the city of Mumbai and its suburbs. The SUHI of all other categories is calculated as the differential mean LST concerning zone C1 (Figure 10).

6. Conclusions

The study concludes that the physical characteristics of various components of the urban fabric, collectively modulate zonal LST, which in turn defines the intensity of SUHI. The physical characteristics like the height of built forms, their footprints on the ground, the proportion of vegetation and the size of land parcels are an outcome of the development control regulations applicable in an area.

It is concluded that the LST has a strong negative correlation *(R = –0.88)* with the FSI (*also known as floor area ratio FAR*). There is a tendency of building more on the ground in the low-rise, low-FSI zones. As the FSI increases and more floors are added, more space is mandatorily left on the ground for the movement of fire vehicles and other services, which in turn relieves more space for vegetation on the ground. Hence the development with a higher FSI is desirable.

SUHII is found to have a strong positive correlation (*R* = 0.968) with the average ground area covered by the BF. Low-rise development consuming more land on the ground is economically viable on the city fringe but as the city grows, these areas become a part of the city core and are converted into un-liveable heat pockets, economically unviable and unsustainable due to the escalated land prices. Therefore, this study provides valuable insight that can prevent such scenarios through timely interventions.

The study concludes that the amount of vegetation has a negative correlation with the SUHI intensities. The larger pockets of well-vegetated surfaces are a good strategy to bring down the overall LST of an area. Small/narrow strips of vegetative surfaces around the building are not an effective strategy to bring down the overall LST. Open spaces with bare ground surfaces exhibit high surface temperatures and therefore elevate the SUHII.

The study supports the findings of previous studies that the roof covering material plays an important role in modulating SUHII by increasing the upwelling thermal radiations. Therefore, cool and vegetated roofs are desirable for mitigating SUHII, especially where more ground is covered by the BFs. Large plot sizes with high FSI/FAR and low ground coverage along with cool and vegetated roof strategies are desirable.

It is recommended that the objective of reducing the intensity of heat islands, by optimizing FSI, ground area covered by building footprints, proportions and configurations of open areas and the guidelines for roofing materials, must be included at the stage of formulation of future development plans and control regulations.

The development proposals in fringe areas/exurbs especially while catering to the spillover city functions, in view to finding economically viable solutions, should be formulated prognosticating the future long-term scenario and prevent them from becoming heat pockets when they merge with the city fabric.

Authors contributions

All authors contributed to the study's conception and design. Material preparation, data collection and analysis were performed by Vandana Tiwari Srivastava, Alok Sharma and Sanjay Singh Jadon. The first draft of the manuscript was written by Vandana Tiwari Srivastava and all authors commented on previous versions of the manuscript. All authors read and approved the final manuscript.

Conflict of interests

The authors declare that there are no conflicts of interest.

References

Agathangelidis, I., Cartalis, C., & Santamouris, M. (2020). Urban morphological controls on surface thermal dynamics: A comparative assessment of major European cities with a focus on Athens, Greece. *Climate, 8*(11), 1–33.
https://doi.org/10.3390/cli8110131

Avdan, U., & Jovanovska, G. (2016). Algorithm for automated mapping of land surface temperature using LANDSAT 8 satellite data. *Journal of Sensors, 2016*, Article 1480307.
https://doi.org/10.1155/2016/1480307

Chen, Y., Yang, J., Yu, W., Ren, J., Xiao, X., & Xia, J. C. (2023). Relationship between urban spatial form and seasonal land surface temperature under different grid scales. *Sustainable Cities and Society, 89*, Article 104374.
https://doi.org/10.1016/j.scs.2022.104374

Climate Data. (n.d.). *Mumbai climate: Average temperature by month, Mumbai water temperature*. Retrieved February 22, 2023, from https://en.climate-data.org/asia/india/maharashtra/mumbai-29/

de Almeida, C. R., Teodoro, A. C., & Gonçalves, A. (2021). Study of the urban heat island (UHI) using remote sensing data/techniques: A systematic review. *Environments*, *8*(10), Article 105. https://doi.org/10.3390/environments8100105

Department of the Interior U.S. Geological Survey. (2016, June). Landsat 8 data users handbook. *Nasa*, *8*, 97. https://landsat.usgs.gov/documents/Landsat8DataUsersHandbook.pdf

Farid, N., Moazzam, M. F. U., Ahmad, S. R., Coluzzi, R., & Lanfredi, M. (2022). Monitoring the impact of rapid urbanization on land surface temperature and assessment of surface urban heat island using Landsat in megacity (Lahore) of Pakistan. *Frontiers in Remote Sensing*, *3*, 1–12. https://doi.org/10.3389/frsen.2022.897397

Gkatzioura, P. E., & Perakis, K. (2022, October 19–21). SES 2022 analysis of Urban Heat Island (UHI) through climate engine and ArcGIS Pro in different cities of Bulgaria. In *SES 2022, Eighteenth International Scientific Conference, Space, Ecology, Safety* (pp. 187–197), Sofia, Bulgaria. https://www.researchgate.net/publication/365374762

Grover, A., & Singh, R. B. (2015). Analysis of urban heat island (UHI) in relation to normalized difference vegetation index (NDVI): A comparative study of Delhi and Mumbai. *Environments*, *2*(2), 125–138. https://doi.org/10.3390/environments2020125

Han, D., An, H., Cai, H., Wang, F., Xu, X., Qiao, Z., Jia, K., Sun, Z., & An, Y. (2023). How do 2D/3D urban landscapes impact diurnal land surface temperature: Insights from block scale and machine learning algorithms. *Sustainable Cities and Society*, *99*, Article 104933. https://doi.org/10.1016/j.scs.2023.104933

Han, D., An, H., Wang, F., Xu, X., Qiao, Z., Wang, M., Sui, X., Liang, S., Hou, X., Cai, H., & Liu, Y. (2022). Understanding seasonal contributions of urban morphology to thermal environment based on boosted regression tree approach. *Building and Environment*, *226*, Article 109770. https://doi.org/10.1016/j.buildenv.2022.109770

He, S., Wang, X., Dong, J., Wei, B., Duan, H., Jiao, J., & Xie, Y. (2019). Three-dimensional urban expansion analysis of valley-type cities: A case study of Chengguan District, Lanzhou, China. *Sustainability*, *11*(20), Article 5663. https://doi.org/10.3390/su11205663

Huang, X., & Wang, Y. (2019). Investigating the effects of 3D urban morphology on the surface urban heat island effect in urban functional zones by using high-resolution remote sensing data: A case study of Wuhan, Central China. *ISPRS Journal of Photogrammetry and Remote Sensing*, *152*, 119–131. https://doi.org/10.1016/j.isprsjprs.2019.04.010

Ishola, K. A., Okogbue, E. C., & Adeyeri, O. E. (2016). A quantitative assessment of surface urban heat islands using satellite multi-temporal data over Abeokuta, Nigeria. *International Journal of Atmospheric Sciences*, *2016*, Article 3170789. https://doi.org/10.1155/2016/3170789

Kalota, D. (2017). Exploring relation of land surface temperature with selected variables using geographically weighted regression and ordinary least square methods in Manipur State, India. *Geocarto International*, *32*(10), 1105–1119. https://doi.org/10.1080/10106049.2016.1195883

Keeratikasikorn, C., & Bonafoni, S. (2018). Urban heat island analysis over the land use zoning plan of Bangkok by means of Landsat 8 imagery. *Remote Sensing*, *10*(3), Article 440. https://doi.org/10.3390/rs10030440

Koko, A. F., Yue, W., Abubakar, G. A., Alabsi, A. A. N., & Hamed, R. (2021). Spatiotemporal influence of land use/land cover change dynamics on surface urban heat island: A case study of Abuja metropolis, Nigeria. *ISPRS International Journal of Geo-Information*, *10*(5), Article 272. https://doi.org/10.3390/ijgi10050272

Leal Filho, W., Wolf, F., Castro-Díaz, R., Li, C., Ojeh, V. N., Gutiérrez, N., Nagy, G. J., Savić, S., Natenzon, C. E., Al-Amin, A. Q., Maruna, M., & Bönecke, J. (2021). Addressing the urban heat islands effect: A cross-country assessment of the role of green infrastructure. *Sustainability*, *13*(2), 1–20. https://doi.org/10.3390/su13020753

Lesado, A. (2018). Clay roofing tile: A cool roof? *Open Journal of Science and Technology*, *1*(1), 1–3. https://doi.org/10.31580/ojst.v1i1.151

Li, F., Sun, W., Yang, G., & Weng, Q. (2019). Investigating spatiotemporal patterns of surface urban heat islands in the Hangzhou Metropolitan area, China, 2000–2015. *Remote Sensing*, *11*(13), Article 1553. https://doi.org/10.3390/rs11131553

Moazzam, M. F. U., Doh, Y. H., & Lee, B. G. (2022). Impact of urbanization on land surface temperature and surface urban heat Island using optical remote sensing data: A case study of Jeju Island, Republic of Korea. *Building and Environment*, *222*, Article 109368. https://doi.org/10.1016/j.buildenv.2022.109368

Mondal, A., Guha, S., & Kundu, S. (2021). Dynamic status of land surface temperature and spectral indices in Imphal city, India from 1991 to 2021. *Geomatics, Natural Hazards and Risk*, *12*(1), 3265–3286. https://doi.org/10.1080/19475705.2021.2008023

Morabito, M., Crisci, A., Guerri, G., Messeri, A., Congedo, L., & Munafò, M. (2021). Surface urban heat islands in Italian metropolitan cities: Tree cover and impervious surface influences. *Science of the Total Environment*, *751*, Article 142334. https://doi.org/10.1016/j.scitotenv.2020.142334

Mukherjee, F., & Singh, D. (2020). Assessing land use–land cover change and its impact on land surface temperature using LANDSAT data: A comparison of two urban areas in India. *Earth Systems and Environment*, *4*(2), 385–407. https://doi.org/10.1007/s41748-020-00155-9

Mumbai Metropolitan Region Development Authority. (n.d.). *Regional plan*. Retrieved February 22, 2023, from https://mmrda.maharashtra.gov.in/planning/regional-plan/final-rp-for-mmr

Naim, Md. N. H., & Kafy, A.-A. (2021). Assessment of urban thermal field variance index and defining the relationship between land cover and surface temperature in Chattogram city: A remote sensing and statistical approach. *Environmental Challenges*, *4*, Article 100107. https://doi.org/10.1016/j.envc.2021.100107

Nor Afzan Buyadi, S., Mohd Naim Wan Mohd, W., & Misni, A. (2014). *Quantifying green space cooling effects on the urban microclimate using remote sensing and GIS techniques*. https://www.researchgate.net/publication/325170006

Ogashawara, I., & Bastos, V. (2012). A quantitative approach for analyzing the relationship between urban heat islands and land cover. *Remote Sensing*, *4*(11), 3596–3618. https://doi.org/10.3390/rs4113596

Oke, T. R. (1982). The energetic basis of the urban heat island. *Quarterly Journal of the Royal Meteorological Society*, *108*(455), 1–24. https://doi.org/10.1002/qj.49710845502

Pan, J. (2016). Area delineation and spatial-temporal dynamics of urban heat island in Lanzhou city, China using remote sensing imagery. *Journal of the Indian Society of Remote Sensing*, *44*(1), 111–127. https://doi.org/10.1007/s12524-015-0477-x

Pandey, A., Mondal, A., Guha, S., Upadhyay, P. K., & Rashmi. (2022a). A seasonal investigation on land surface temperature and spectral indices in Imphal City, India. *Journal of Landscape Ecology*, *15*(3), 1–18. https://doi.org/10.2478/jlecol-2022-0015

Pandey, A., Mondal, A., Guha, S., Upadhyay, P. K., & Singh, D. (2022b). Land use status and its impact on land surface temperature in Imphal city, India. *Geology, Ecology, and Landscapes*. https://doi.org/10.1080/24749508.2022.2131962

Pandey, A., Mondal, A., Guha, S., Upadhyay, P. K., & Singh, D. (2023). A long-term analysis of the dependency of land surface temperature on land surface indexes. *Papers in Applied Geography*, *9*(3), 279–294.
https://doi.org/10.1080/23754931.2023.2187314

Parvez, I. M., Aina, Y. A., & Balogun, A.-L. (2021). The influence of urban form on the spatiotemporal variations in land surface temperature in an arid coastal city. *Geocarto International*, *36*(6), 640–659.
https://doi.org/10.1080/10106049.2019.1622598

Rahaman, S., Jahangir, S., Haque, M. S., Chen, R., & Kumar, P. (2021). Spatio-temporal changes of green spaces and their impact on urban environment of Mumbai, India. *Environment, Development and Sustainability*, *23*(4), 6481–6501.
https://doi.org/10.1007/S10668-020-00882-z

Roy, B., & Kasemi, N. (2021). Monitoring urban growth dynamics using remote sensing and GIS techniques of Raiganj Urban Agglomeration, India. *Egyptian Journal of Remote Sensing and Space Science*, *24*(2), 221–230.
https://doi.org/10.1016/j.ejrs.2021.02.001

Sajjad, S. H., Shirazi, S. A., Ahmed Khan, M., & Raza, A. (2009). Urbanization effects on temperature trends of Lahore during 1950-2007. *International Journal of Climate Change Strategies and Management*, *1*(3), 274–281.
https://doi.org/10.1108/17568690910977483

Schwarz, N., Schlink, U., Franck, U., & Großmann, K. (2012). Relationship of land surface and air temperatures and its implications for quantifying urban heat island indicators–An application for the city of Leipzig (Germany). *Ecological Indicators*, *18*, 693–704. https://doi.org/10.1016/j.ecolind.2012.01.001

Shahfahad, Rihan, M., Naikoo, M. W., Ali, M. A., Usmani, T. M., & Rahman, A. (2021). Urban heat island dynamics in response to land-use/land-cover change in the coastal city of Mumbai. *Journal of the Indian Society of Remote Sensing*, *49*(9), 2227–2247. https://doi.org/10.1007/s12524-021-01394-7

Shahfahad, Talukdar, S., Rihan, M., Hang, H. T., Bhaskaran, S., & Rahman, A. (2022). Modelling urban heat island (UHI) and thermal field variation and their relationship with land use indices over Delhi and Mumbai metro cities. *Environment, Development and Sustainability*, *24*(3), 3762–3790.
https://doi.org/10.1007/S10668-021-01587-7

Sharma, R., Ghosh, A., & Joshi, P. K. (2013). Analysing spatio-temporal footprints of urbanization on environment of Surat city using satellite-derived bio-physical parameters. *Geocarto International*, *28*(5), 420–438.
https://doi.org/10.1080/10106049.2012.715208

Singh, R. B., Grover, A., & Zhan, J. (2014). Inter-seasonal variations of surface temperature in the urbanized environment of Delhi using Landsat thermal data. *Energies*, *7*(3), 1811–1828.
https://doi.org/10.3390/en7031811

Suresh, S., Ajay Suresh, V., & Mani, K. (2016). Estimation of land surface temperature of high range mountain landscape of Devikulam Taluk using Landsat 8 data. *International Journal of Research in Engineering and Technology*, *5*(1), 92–96.
https://doi.org/10.15623/ijret.2016.0501017

Unger, J., Gál, T., Rakonczai, J., Mucsi, L., Szatmári, J., Tobak, Z., van Leeuwen, B., & Fiala, K. (2009, June 29–July 3). *Air temperature versus surface temperature in urban environment* [Conference presentation]. The Seventh International Conference on Urban Climate, Okohama, Japan.

Xu, H. (2015). Assessment of changes in green space of Nanjing city using 1998 and 2007 Landsat satellite data. *Open House International*, *40*(4), 63–70.
https://doi.org/10.1108/ohi-04-2015-b0011

Zhang, R., Yang, J., Ma, X., Xiao, X., & Xia, J. (Cecilia). (2023). Optimal allocation of local climate zones based on heat vulnerability perspective. *Sustainable Cities and Society*, *99*, Article 104981. https://doi.org/10.1016/j.scs.2023.104981